

Shapiro steps in charge-density-wave states driven by ultrasound

Michiyasu Mori¹ and Sadamichi Maekawa^{1,2,3}

¹Advanced Science Research Center, Japan Atomic Energy Agency, Tokai, Ibaraki 117-1195, Japan

²RIKEN Center for Emergent Matter Science, Wako 351-0198, Japan

³Kavli Institute for Theoretical Sciences, University of Chinese Academy of Sciences, Beijing 100049, China

(Dated: January 10, 2024)

We show that an ultrasound can induce the Shapiro steps (SS) in the charge-density-wave (CDW) state. When an ultrasound with frequency ω is applied with a dc bias-voltage, the SS appear at the current $I \propto n\omega$ with integer n . Two couplings between the CDW and an ultrasound constitute even and odd multiples of SS, respectively. Although an ac voltage with frequency ω also induces the SS at $I \propto n\omega$, the ultrasound will enhance the odd multiples more strongly than the even ones. This is the difference between the ultrasound and the ac voltage. Since the dV/dI shows sharp peaks due to the SS, the drastic changes in the I - V curve will be applied to a highly sensitive detector of ultrasound.

The charge-density-wave (CDW) is a macroscopic quantum state with twice of the Fermi wave vector ($2k_F$) induced by pairing of electrons and holes. Below a critical temperature of the Peierls transition T_c , the CDW is formed by the electron-phonon interaction so as to open a semiconducting gap at the FS and leads to an increase of resistivity [1]. The CDW is pinned by impurities and/or commensurability to the lattice. When an applied electric field exceeds a threshold, the CDW is depinned and starts to slide through the lattice adding to the conductivity [2–7]. Remarkable transport properties were observed in transition metal trichalcogenides such as NbSe₃ and TaS₃ [8–12]. Above the threshold dc field, a current by the sliding of CDW contains not only a dc but also oscillating components referred to as narrow-band noise [13–18]. When a dc and an ac voltage are applied together, steps appear in a I - V curve [13–18]. These steps are induced by phase locking of an external frequency with an internal one. This mechanism is same to the Shapiro steps (SS) in a Josephson junction of superconductors. Below, the steps of a I - V curve in the CDW state will be called ‘‘Shapiro steps’’ (SS).

The ultrasound has a rich variety of applications. The ultrasonography is used for biomedical diagnostics in hospitals to see the inside of our body or to destroy tumors. A touch sensor using an ultrasound is installed in some monitors. The symmetry of superconducting order parameters were studied by the ultrasound attenuation [19, 20]. On a surface of ferromagnet, a surface acoustic wave is used to control a spin current [21–23]. Recently, an electrical control of surface acoustic wave has been realized toward quantum information technology [24]. The ultrasound does not radiate into free-space in contrast to the electromagnetic waves, and hence allows coherent information processing and manipulation with negligible cross talk between devices and with their environments [25]. The ultrasound is generated and detected by a piezoelectric material such as lithium niobate. Improved sensitivity to the ultrasound will make its application much wider to quantum information technology.

In this paper, we show that an ultrasound can induce the SS in the CDW state. When an ultrasound with frequency ω is applied with a dc bias-voltage, the SS appear at the current $I \propto n\omega$ with integer n . An ac voltage with frequency ω also

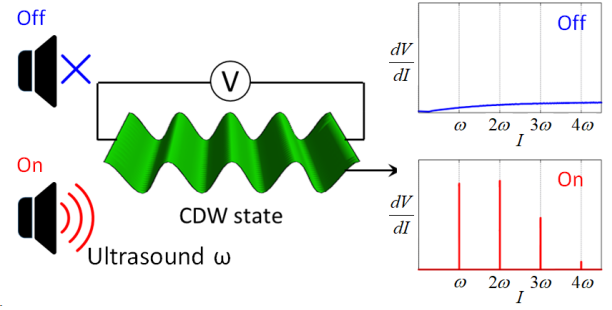


FIG. 1. Schematic diagram of ultrasound detection using a CDW state. The central figure indicates that the CDW state is biased by a voltage. In the upper half, when the ultrasound is off, the dV/dI is monotonic as a function of I . In the lower half, when the ultrasound with frequency ω is applied, the peak structures appear at ω multiples.

induces the SS at $I \propto n\omega$. Using the ultrasound, however, the odd multiples of SS will be enhanced rather than the even ones depending on conditions due to two couplings of CDW to an ultrasound; one contributes to even multiples and another one does to odd multiples. This is the difference between the ultrasound and the ac voltage. Since the dV/dI shows sharp peaks due to the SS (See Fig. 1), the drastic changes in the I - V curve will be applied to a highly sensitive detector of ultrasound. Recently, the SS by mechanical vibration has been reported [26].

The charge density in a CDW state $\rho(x, t)$ is written by,

$$\rho(x, t) = \rho_0 + \rho_1 \cos [2k_F x + \theta(x, t)], \quad (1)$$

where averaged charge density ρ_0 and magnitude of $2k_F$ -oscillation ρ_1 are constant. The dynamical behavior at low energies is given by,

$$\mathcal{L}_0 = \frac{1}{4\pi v'} \int dx \{ [\partial_t \theta(x, t)]^2 - v^2 [\partial_x \theta(x, t)]^2 \}, \quad (2)$$

where $v' \equiv v^2/v_F$ with Fermi velocity v_F and v is velocity of Goldstone mode in the CDW state [5]. In one-dimensional electron systems, $\theta(x, t)$ is related to fermionic

operators $\psi_{s\pm}$ of electrons using the bosonization given by, $\psi_{s\pm} \sim \exp(\pm ik_F x \pm \theta_{s\pm})$ so as to $\theta(x, t) = \sum_s \theta_{s+} + \theta_{s-}$ with spin s [27–30]. These equations suggest that θ means fluctuation of electron density around Fermi surface. Considering $k_F = (2\pi/L)(N/2)$ with system size L and number of electrons N , k_F corresponds to the electron density $N/L \equiv n$. Then, fluctuation of n is given by $(1/\pi)[\partial\theta(x, t)/\partial x]$. The continuity equation $\partial_t n + \partial_x j = 0$ defines the current $j = -(1/\pi)[\partial\theta(x, t)/\partial t]$.

Pinning of CDW is the key for the transport properties. Below, we will discuss a single impurity model. An impurity potential at $x = 0$ is given by,

$$U_{\text{imp}} = -u_0\rho_1 \int dx \cos [Qx + \theta(x, t)] \delta(x), \quad (3)$$

$$= -u_0\rho_1 \cos \theta, \quad (4)$$

where $Q \equiv 2k_F$, $\theta \equiv \theta(x = 0, t)$, $u_0 > 0$ and $\rho_1 > 0$. When an ultrasound or a surface acoustic wave is applied, the impurity is shifted from its original position and add the energy given by,

$$U_{\text{snd}} = u_0\rho_1 \int dx \cos [Qx + \theta(x, t)] [\delta(x - \xi(t)) - \delta(x)], \quad (5)$$

$$\sim -u_0\rho_1 \sin \theta \cdot [Q + \partial\theta/\partial x] \cdot \xi(t), \quad (6)$$

where $\partial\theta/\partial x \equiv \partial\theta(x, t)/\partial x|_{x \rightarrow \pm R_0}$ [31]. At the impurity site, $x = 0$, the spatial variation of $\theta(x, t)$ is singular and its derivative is not continuous [32]. The right (left) derivative of $\theta(x, t)$ at the impurity site will be negative (positive) so as to fix the sign of $\partial\theta/\partial x \cdot \xi(t)$. For $Q \cdot \xi(t) \equiv \eta \cos(\omega t)$, the pinning potential and the coupling to an ultrasound are given by,

$$U = U_{\text{imp}} + U_{\text{snd}}, \quad (7)$$

$$= -u_0\rho_1 [\cos \theta + \sin \theta \cdot d(t)], \quad (8)$$

$$d(t) \equiv \eta (\chi \cos \omega t + \lambda |\cos \omega t|), \quad (9)$$

where $\chi = 1$, and $\lambda \equiv |\partial\theta/\partial x|/Q > 0$. In Eq. (9), the first term will be dominant in most cases, since λ corresponds to a fluctuation of electron density per site or unit cell δn . It is usually less than 1, i.e., $\lambda \sim \delta n < 1$. Below, $\eta = 1$ is imposed for brevity and the following results do not change qualitatively. The magnitude of oscillation at impurity site is proportional to η , which can be controlled by an input power of ultrasound.

The single impurity model can cover some essential parts of CDW transport properties. This is the limit of strong pinning. When the pinning is weak so that the single impurity cannot pin the phase of the CDW, the pinning potential is determined by a balance between the increase in kinetic energy due to change of charge density, i.e., the second term of Eq. (2), and an energy gain from phase-dependent impurity pinning energy [6, 7]. These are characterized by the pinning frequency in the optical conductivity [6, 7]. The important feature of the impurity pinning is the spatial distortions of the phase in the ground state due to the random distribution of impurities. However, if the quantity of interest is not sensitive to such spatial variation, the pinning will be described by an

averaged potential proportional to $\cos \theta(x, t)$, where $\theta(x, t)$ is an averaged phase within a domain determined by impurity distribution [33]. Hence, the above discussion will be valid even in a weak pinning region.

The dynamics of phase motion can be treated classically, since electrons move together with lattice distortion and then the effective mass of CDW is large. Similar to the SS in a Josephson junction of superconductors, the transport properties of CDW can be calculated by,

$$\alpha \frac{d^2\theta}{dt^2} + \beta \frac{d\theta}{dt} + U'(\theta) = F(t), \quad (10)$$

with $U'(\theta) = dU/d\theta$. Equation (10) is interpreted as the acceleration $\alpha d^2\theta/dt^2$ by the effective driving force, $F_{\text{eff}} = F(t) - U'(\theta)$, with the friction term $\beta d\theta/dt$. In an overdamped region, $\alpha \sim 0$, the first term in Eq. (10) is neglected. When a CDW is driven by an ultrasound, the transport properties are determined by,

$$\beta \frac{d\theta}{dt} + u_0\rho_1 [\sin \theta + \cos \theta \cdot d(t)] = f_{dc}, \quad (11)$$

where f_{dc} corresponds to a bias dc voltage. Below, we will use the following parametrization,

$$\frac{d\theta}{dt} + U'(\theta) = V, \quad (12)$$

$$U'(\theta) = A [\sin \theta + \cos \theta \cdot d(t)]. \quad (13)$$

The current $I \equiv \pi j$ is calculated by averaging of $\partial\theta(t)/\partial t$ in time as,

$$I = -\frac{1}{T} \int_0^T dt \left(\frac{\partial\theta(t)}{\partial t} \right). \quad (14)$$

Solving Eqs. (12) and (14), the I - V curves are obtained as shown in Fig. 2 with $\omega = 0.25$, $\chi = 1.0$ and $\lambda = 1.0$ (orange), 0.5 (blue), and 0.0 (red). The SS appear at $I/\omega = n$ for $\lambda = 1.0$ and 0.5. For $\lambda = 0.0$, however, the SS appear at only odd multiples, i.e., $I/\omega = 2n+1$, and even multiples are suppressed. This is a crucial difference between an ultrasound and an ac voltage biases. When the system is driven by the ac voltage, the equation of motion is given by [14, 15],

$$\frac{d\theta}{dt} = V - A \sin \theta - \eta_{ac} \cos(\omega t). \quad (15)$$

Solving Eq. (15), the I - V curves are obtained as shown in Fig. 3 with $\omega = 0.25$ and $\eta_{ac} = 0.5$ (red), 0.25 (blue), and 0.0 (black). The SS appear at $I/\omega = n$ similar to a Josephson junction of superconductors. In the case of Eq. (15), assuming $\theta = at - b \sin(\omega t)$ with constants a and b , and using the relation, $e^{iz \sin \theta} = \sum_n J_n(z) e^{in\theta}$, with Bessel function $J_n(z)$, the potential term is transformed as, $\sin \theta = \text{Im}[\sum_n J_n(b) e^{i(a-n\omega)t}]$. When $a = n\omega$ is satisfied, the time-average of $\sin \theta$ is independent of time and leads to the SS. In the ultrasound bias Eq. (13), since another potential term is multiplied to the oscillation such as, $\sin \theta \cos \omega t$, analytical

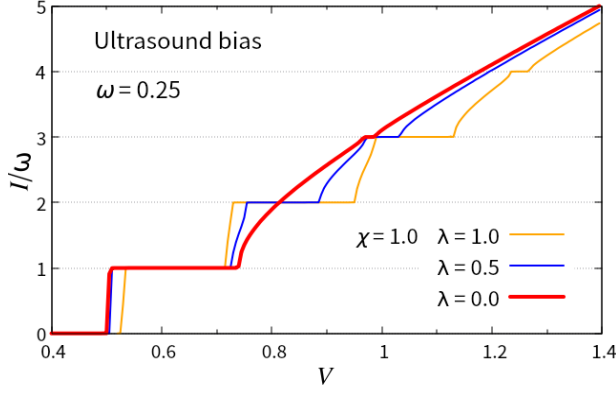


FIG. 2. The I - V curve driven by ultrasound with $\omega = 0.25$, $A = 0.5$, $\chi = 1.0$, and $\lambda = 1.0$ (orange), 0.5 (blue), and 0.0 (red). The SS appear at $I/\omega = n$ with integer n except for $\lambda = 0.0$, where only odd multiples appear.

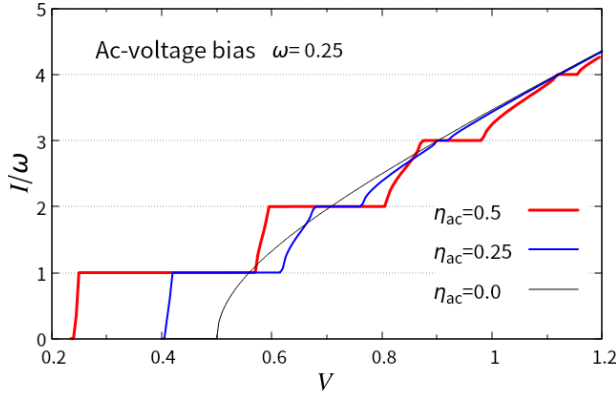


FIG. 3. The I - V curve driven by an ac voltage with $\omega = 0.25$, $A = 0.5$, and $\eta_{ac} = 0.5$ (red), 0.25 (blue) curve. The black curve is without ac voltage. The steps appear at $I/\omega = n$ with integer n .

estimation of the SS is difficult. However, using the guess, $\theta = at - b \cos(\sin \omega t)$, the potential term is written as, $\sin \theta = \text{Im} \left[\sum_{n>0,m} J_n(b) J_m(n) (1 + (-1)^m) e^{i(a-m\omega)t - in\pi/2} \right]$. Then, the SS appear at $a = m\omega$ with even multiples. When $\lambda=0$, the oscillating term in Eq. (13) is proportional to $\cos(\theta - \omega t) + \cos(\theta + \omega t)$. Hence, another guess $\theta \pm \omega t = at - b \cos(\sin \omega t)$ could be possible, and the SS appear at odd multiples as shown in Fig. 2.

The black line in Fig. 3 shows the threshold $V = A$, at which the solution changes its behavior. At $\eta_{ac} = 0$, Eq. (15) is analytically solved as, $V \tan(\theta(t)/2) = A + (V^2 - A^2)^{1/2} \tan[(V^2 - A^2)^{1/2} t/2]$. For $V < A$, the solution is monotonously merging to a constant, whereas, for $V > A$, the solution oscillatory increases or decreases with time. Considering Eq. (14), the increase or decrease of θ in time leads to a finite value of I . This suggests that the solution at the SS does not change its

gradient due to the phase-locking.

In Fig. 2, without the λ -term in Eq. (9), the SS appear only at odd multiples. On the other hand, only with the λ -term, i.e., $\chi = 0.0$, the I - V curves are plotted in Fig. 4 for $\lambda = 1.0$ (green) and 0.5 (purple). Notably, the SS appear at even multiples, i.e.

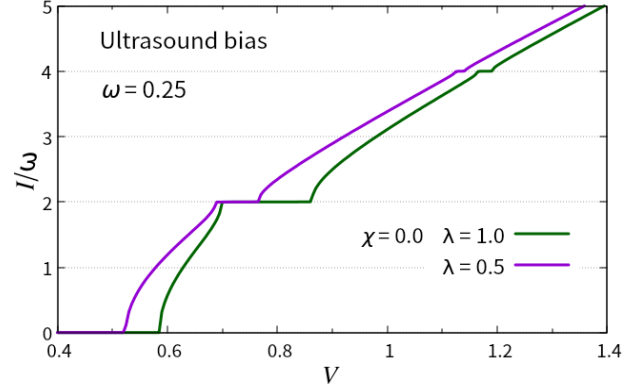


FIG. 4. The I - V curve driven by ultrasound for $\chi = 0.0$ with $\omega = 0.25$, $A = 0.5$, and $\eta = 1.0$ (green), 0.5 (purple) curve. The SS appear at $I/\omega = 2n$ with integer n .

$I/\omega = 2n$, which is in sharp contrast to Fig. 2. The λ -term in Eq. (9), $\cos \theta |\cos \omega t|$, is not equivalent to $\cos(\theta - \omega t) + \cos(\theta + \omega t)$ due to $|\cos \omega t|$. Hence, $\theta = at - b \cos(\sin \omega t)$ will be one of possibilities of even multiples. Another one is due to that the external force proportional to $|\cos \omega t|$ is practically equal to 2ω -oscillation.

We have found that an ultrasound have two ways to drive the CDW state, i.e., χ - and λ -terms in Eq. (9), which induces odd and even multiples in the SS, respectively. Considering those magnitudes of couplings, the odd multiples will dominate the I - V curves. This will be useful to distinguish the ultrasound contribution from an electromagnetic one. For example, when an ultrasound change a dielectric constant of a sample, the electromagnetic field would be simultaneously applied together with the ultrasound. In this case, the SS appear all of integer multiples as $I/\omega = n$. If the induced electromagnetic field becomes weak, the step-width at even multiples will be suppressed. In Fig. 5, the step-width at $I/\omega = 1$ and 2 are plotted as a function of λ for $\chi = 1.0$. The step-width at $I/\omega = 1$ (green) slightly decreases with λ , whereas the step-width at $I/\omega = 2$ (red) rapidly increases from zero. Since λ is proportional to the density fluctuation, λ will be less than 1 and hence the odd multiples such as $I/\omega = 1$ will be clearly observed rather than even ones. The inset of Fig. 5 shows the I - V curve (blue) and its derivative dV/dI (black) for $\lambda = 0.5$. The peaks corresponding to the SS in the I - V curve appear at $I/\omega = n$ with integer n . Here, we consider the case that the dV/dI is measured around a bias voltage such as $V = 0.8$. We will see the sharp peak in dV/dI at $I/\omega = 1$, only when an ultrasound is applied. In addition, this change will be quite fast and drastic similar to the Josephson junction of supercon-

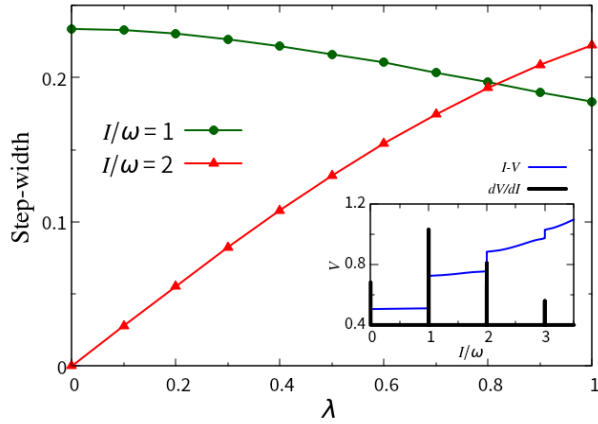


FIG. 5. The λ -dependence of the step-width at $I/\omega = 1$ (green) and 2 (red) with $\omega = 0.25$, $A = 0.5$, and $\chi = 1.0$. The inset shows the I - V curve (blue), which is same to that in Fig. 2, and its derivative dV/dI (black). The peaks corresponding to the steps in the I - V curve appear at $I/\omega = n$ with integer n .

ductors. Hence, the SS in the CDW state will work to detect ultrasounds with high sensitivity.

We have so far discussed the SS in the overdamped region. To check the effect of the kinetic term, i.e., the first term in Eq. (10), the following equation is solved to calculate the I - V curve,

$$\gamma \frac{d^2\theta}{dt^2} + \frac{d\theta}{dt} + U'(\theta) = V. \quad (16)$$

The results are shown in Fig. 6 for $\omega = 0.25$, $A = 0.5$, $\chi = \lambda$ =1.0, and $\gamma = 0.5$ (red), 1.0 (blue), and 2.0 (green). Obvi-

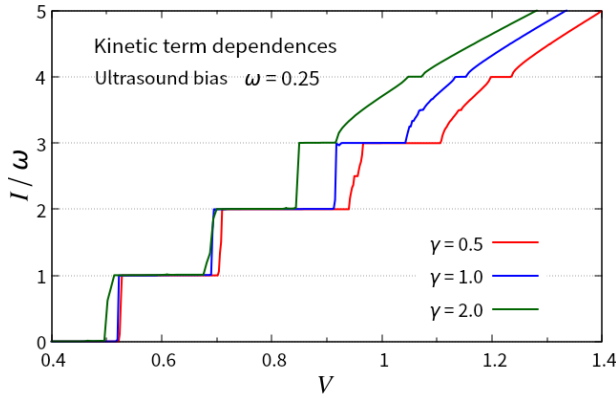


FIG. 6. The I - V curve driven by ultrasound with $\omega = 0.25$, $A = 0.5$, $\chi = \lambda = 1.0$, and $\gamma = 0.5$ (red), 1.0 (blue), and 2.0 (green).

ously, the SS appear at $I/\omega = n$ independently of the kinetic term. Hence, the SS in the CDW state will sensitively respond to the ultrasound, even if the kinetic term exists. In the cases of $\gamma = 0.5$ and 1.0, the I - V curves show a tiny sub-harmonics

at $I/\omega = 2.5$ and 3.5, respectively. The overdamped model with a single impurity cannot explain the subharmonic steps, i.e., $I/\omega \propto n/m$, whereas the kinetic term changes the matching condition of the phase locking and can induce the subharmonic steps [34]. Some materials clearly show subharmonic steps, whose magnitude might not be explained only by the kinetic term [16, 17]. Another possibility to reproduce the subharmonic steps is multiple impurities in the overdamped model [35–37]. In this case, the subharmonic steps also becomes visible comparable to the harmonic steps. On the other hand, Bardeen proposed a non-sinusoidal potential, in which an averaged impurity distribution is periodic and the phase of CDW state tunnels between two stable states [18, 38, 39]. The multiple impurities and the non-sinusoidal potential are beyond our scope in this paper. Those will be studied in the near future.

We have shown that an ultrasound can induce the SS in the CDW state. When an ultrasound with frequency ω is applied with a dc bias-voltage, the SS appear at the current $I \propto n\omega$ with integer n . Two couplings between the CDW and an ultrasound constitute even and odd multiples of SS, respectively. Although an ac voltage with frequency ω also induces the SS at $I \propto n\omega$, the ultrasound will enhance the odd multiples more strongly than the even ones. This is the difference between the ultrasound and the ac voltage. Since the dV/dI shows sharp peaks due to the SS (See Fig. 1), the drastic changes in the I - V curve will be applied to a highly sensitive detector of ultrasound.

We would like to thank Prof Niimi and Fujiwara for valuable discussions about the experiments on SAW in 1D CDW materials. Thanks are also to Prof Matsukawa for his important suggestions and valuable discussions. This work was supported by JSPS Grant Nos. JP20K03810 and JP21H04987, and the inter-university cooperative research program (No. 202012-CNKXX-0008) of the Center of Neutron Science for Advanced Materials, Institute for Materials Research, Tohoku University. A part of the computations was performed on supercomputers at the Japan Atomic Energy Agency. S.M. is supported by JST CREST Grant (Nos. JPMJCR19J4, JPMJCR1874, and JPMJCR20C1) and JSPS KAKENHI (nos. 17H02927 and 20H01865) from MEXT, Japan.

- [1] R. E. Peierls, "*Quantum Theory of Solids*", Oxford University Press, Oxford (1955).
- [2] H. Fröhlich, Proc. R. Soc. A **223**, 296 (1954).
- [3] D. Allender, J. W. Bray, and J. Bardeen, Phys. Rev. B **9**, 119 (1974).
- [4] P. A. Lee, T. M. Rice, and P. W. Anderson, Solid State Commun. **14**, 703 (1974).
- [5] H. Fukuyama, J. Phys. Soc. Jpn. **41**, 513 (1976).
- [6] H. Fukuyama and P. A. Lee, Phys. Rev. B **17**, 535 (1978).
- [7] P. A. Lee and T. M. Rice, Phys. Rev. B **19**, 3970 (1979).
- [8] P. Monceau, N. P. Ong, A. M. Portis, A. Meerschaut, and J.

- Rouxel, Phys. Rev. Lett. **37**, 602 (1976).
- [9] T. Takoshima, M. Ido, K. Tsutsumi, T. Sambongi, S. Honma, K. Yamaya, and Y. Abe, Solid State Commu. **35**, 911 (1980).
- [10] P. Monceau, J. Richard, and M. Renard, Phys. Rev. Lett. **45**, 43 (1980).
- [11] "Electronic Properties of Inorganic Quasi-One-Dimensional Materials I & II", Ed. P. Monceau, D. Reidel Publishing Company, Dordrecht, Holland (1985).
- [12] G. Grüner and A. Zettl, Phys. Rep. **119**, 117 (1985).
- [13] R. M. Fleming and C. C. Grimes, Phys. Rev. Lett. **42**, 1423 (1979).
- [14] G. Grüner, A. Zawadowski, and P. M. Chaikin, Phys. Rev. Lett. **46**, 511 (1981).
- [15] P. Monceau, J. Richard, and M. Renard, Phys. Rev. B **25**, 931 (1982).
- [16] S. E. Brown, G. Mozurkewich, and G. Grüner, Phys. Rev. Lett. **52**, 2277 (1984).
- [17] S. E. Brown, G. Mozurkewich, G. Grüner, and A. Zawadowski, Solid State Commu. **54**, 23 (1985).
- [18] R. E. Thorne, J. R. Tucker, J. Bardeen, S. E. Brown, and G. Grüner, Phys. Rev. B **33**, 7342 (1986).
- [19] T. Tsuneto, Phys. Rev. **121**, 402 (1961).
- [20] M. Sigrist and K. Ueda, Rev. Mod. Phys. **63**, 239 (1991).
- [21] S. Maekawa and M. Tachiki, AIP Conf. Proc. **29**, 542 (1976).
- [22] D. Kobayashi, T. Yoshikawa, M. Matsuo, R. Iguchi, S. Maekawa, E. Saitoh, and Y. Nozaki, Phys. Rev. Lett. **119**, (2017).
- [23] M. Xu, K. Yamamoto, J. Puebla, K. Baumgaertl, B. Rana, K. Miura, H. Takahashi, D. Grundler, S. Maekawa, and Y. Otani, Science Advances **6**, eabb1724 (2020).
- [24] L. Shao, D. Zhu, M. Colangelo, D. Lee, N. Sinclair, Y. Hu, P. T. Rakich, K. Lai, K. K. Berggren, and M. Lončar, Nat. Electron. **5**, 348 (2022).
- [25] M. Maldovan, Nature **503**, 209 (2013).
- [26] M. V. Nikitin, S. G. Zybtsev, V. Ya. Pokrovskii, and B. A. Loginov, Appl. Phys. Lett. **118**, 223105 (2021).
- [27] S. Tomonaga, Prog. Theor. Phys. **5**, 544 (1950).
- [28] J. M. Luttinger, J. Math. Phys. **4**, 1154 (1963).
- [29] J. Sólyom, Adv. Phys. **28**, 201 (1979).
- [30] F. D. M. Haldane, J. Phys. C: Solid State Phys. **14**, 2585 (1981).
- [31] Y. Nagaoka, Progress of Theoretical Physics **26**, 589 (1961).
- [32] N. Teranishi and R. Kubo, J. Phys. Soc. Jpn. **47**, 720 (1979).
- [33] H. Fukuyama and H. Takayama, "Electronic Properties of Inorganic Quasi-One-Dimensional Materials I", pp. 41-104, Ed. P. Monceau, D. Reidel Publishing Company, Dordrecht, Holland (1985).
- [34] M. Ya. Azbel and P. Bak, Phys. Rev. B **30**, 3722 (1984).
- [35] H. Matsukawa and H. Takayama, Synthetic Metals **19**, 7 (1987).
- [36] H. Matsukawa and H. Takayama, Jpn. J. Appl. Phys. **26**, 601 (1987).
- [37] H. Matsukawa, J. Phys. Soc. Jpn. **56**, 1522 (1987).
- [38] J. Bardeen, Phys. Rev. Lett. **55**, 1010 (1985).
- [39] J. Bardeen, "Electronic Properties of Inorganic Quasi-One-Dimensional Materials I", pp. 105-123, Ed. P. Monceau, D. Reidel Publishing Company, Dordrecht, Holland (1985).